

# CONSTITUTIVE MATERIAL MODEL OF FIBER-REINFORCED COMPOSITES AT FINITE STRAINS IN COMSOL MULTIPHYSICS

*Hoang Sy Tuan, B. Marvalova*

Technical University of Liberec, Czech Republic

## Abstract

**This paper presents the Comsol Multiphysics implementation of anisotropic hyperelastic material models for the two-dimensional stress and deformation response of fiber-reinforced composites that experience finite strains. The composites are composed of rubber matrix which is reinforced by one or two families of fibers so that the mechanical properties of the composites depend on the fiber directions. In order to clearly show the good performance of the constitutive model, we present 2D numerical simulations of a stretched laminated rectangular plate with a hole.**

## 1 Introduction

The fiber-reinforced rubber composites so called “soft composites” are formed by cords with high tensile strength reinforcing an elastomer. Typical areas of application are tires, conveyer belts or pneumatic shock absorbers. The physical description of the industrial products mentioned can be extended to biomaterials which often exhibit an anisotropic microstructure. Therefore, constitutive models for bones or soft living tissues such as blood vessels, tendons and ligaments belong to the same class as the artificially produced material. These composites can be submitted to large deformations so the structural model for their mechanical behaviour is formulated within the framework of nonlinear continuum mechanics.

The goal of the present paper is the implementation of the hyperelastic model of fiber-reinforced composites at finite strains into Comsol Multiphysics. We use a particular anisotropic Helmholtz free-energy function described by Holzapfel [1] which allows to model a composite in which a matrix material is reinforced by families of fibers, and hence the mechanical properties of this kind of composites depend on preferred fiber directions. The description of the constitutive model is given with respect to the reference undeformed configuration.

## 2 Constitutive equations of anisotropic hyperelasticity

To describe the fiber reinforced composites at finite strains the Helmholtz free energy function  $\Psi$  is proposed [1,2] which depends not only on the deformation gradient  $F$  but also on the fiber directions.

The free energy for the material with one family of fiber is:

$$\Psi = \Psi(\mathbf{C}, \mathbf{A}_0), \quad (1)$$

where  $\mathbf{C}$  is the right Cauchy-Green deformation tensor,  $\mathbf{A}_0 = \mathbf{a}_0 \otimes \mathbf{a}_0$  is the structural tensor,  $\mathbf{a}_0$  is a unit vector which denotes the fiber direction,  $|\mathbf{a}_0| = 1$ .

The free energy can be written in terms of the invariants of the tensors  $\mathbf{C}$  and the fiber vector  $\mathbf{a}_0$

$$\Psi = \Psi \left[ I_1(\mathbf{C}), I_2(\mathbf{C}), I_3(\mathbf{C}), I_4(\mathbf{C}, \mathbf{a}_0), I_5(\mathbf{C}, \mathbf{a}_0) \right] \quad (2)$$

The first three invariants denote the isotropic matrix material contribution, next two are the contribution of fiber material.

For the two families of fibers, the free energy is written analogically as:

$$\Psi = \Psi(\mathbf{C}, \mathbf{A}_0, \mathbf{B}_0), \quad (3)$$

where  $\mathbf{A}_0 = \mathbf{a}_0 \otimes \mathbf{a}_0$  and  $\mathbf{B}_0 = \mathbf{b}_0 \otimes \mathbf{b}_0$  are the structural tensors of the two fiber directions.

The free energy denoted in terms of the invariants:

$$\Psi = \Psi \left[ I_1(\mathbf{C}), I_2(\mathbf{C}), I_3(\mathbf{C}), I_4(\mathbf{C}, \mathbf{a}_0), I_5(\mathbf{C}, \mathbf{a}_0), I_6(\mathbf{C}, \mathbf{b}_0), I_7(\mathbf{C}, \mathbf{b}_0), I_8(\mathbf{C}, \mathbf{a}_0, \mathbf{b}_0) \right] \quad (4)$$

where

$$\begin{aligned} I_1(\mathbf{C}) &= \text{tr}(\mathbf{C}), & I_2(\mathbf{C}) &= \frac{1}{2} \left[ (\text{tr} \mathbf{C})^2 - \text{tr}(\mathbf{C}^2) \right], & I_3(\mathbf{C}) &= \det(\mathbf{C}), \\ I_4(\mathbf{C}, \mathbf{a}_0) &= \mathbf{a}_0 \cdot \mathbf{C} \mathbf{a}_0, & I_5(\mathbf{C}, \mathbf{a}_0) &= \mathbf{a}_0 \cdot \mathbf{C}^2 \mathbf{a}_0, & I_6(\mathbf{C}, \mathbf{b}_0) &= \mathbf{b}_0 \cdot \mathbf{C} \mathbf{b}_0, \\ I_7(\mathbf{C}, \mathbf{b}_0) &= \mathbf{b}_0 \cdot \mathbf{C}^2 \mathbf{b}_0, & I_8(\mathbf{C}, \mathbf{b}_0) &= (\mathbf{a}_0 \cdot \mathbf{b}_0) \mathbf{a}_0 \cdot \mathbf{C} \mathbf{b}_0. \end{aligned} \quad (5)$$

For the slightly compressible material the free energy can be decoupled to the volumetric, isochoric and anisotropic parts:

$$\Psi = \Psi_{\text{vol}}(J) + \Psi_{\text{iso}}(\bar{I}_1, \bar{I}_2) + \Psi_{\text{ani}}(\bar{I}_\alpha), \quad (6)$$

where  $\alpha = 4, 5$  for the one family of fiber and  $\alpha = 4, 5, 6, 7, 8$  for the two families of fibers,  $\Psi_{\text{vol}}$ ,  $\Psi_{\text{iso}}$  and  $\Psi_{\text{ani}}$  are the volumetric, isotropic and anisotropic deviatoric part, respectively,  $J$  is the ratio of the deformed elastic volume,  $J = \det(\mathbf{F})$ ,  $\bar{I}_1, \bar{I}_2$  and  $\bar{I}_\alpha$  are the modified corresponding invariants:

$$\bar{I}_1 = J^{-2/3} I_1, \quad \bar{I}_2 = J^{-4/3} I_2, \quad \bar{I}_\alpha = J^{-2/3} I_\alpha \text{ for } \alpha=4,6,8, \quad \bar{I}_\alpha = J^{-4/3} I_\alpha \text{ for } \alpha=5,7. \quad (7)$$

The constitutive equation for the second Piola-Kirchhoff stress  $\mathbf{S}$  is obtained from the free energy by differentiation with respect to  $\mathbf{C}$  by means of the chain rule.  $\mathbf{S}$  is expressed in following form:

$$\mathbf{S} = 2 \frac{\partial \Psi}{\partial \mathbf{C}} = \mathbf{S}_{\text{vol}} + \mathbf{S}_{\text{iso}} + \mathbf{S}_{\text{ani}} \quad (8)$$

### 3 Some forms of the free energy function

Numerous specific forms of the strain energy function to describe the elastic properties of incompressible as well as compressible materials have been proposed in literature. We review here some forms which are frequently employed within the constitutive theory of finite elasticity and which we used in our finite element calculus.

#### Volumetric part of strain energy function

The simplest form of the volumetric function  $\Psi_{vol}(J)$ :

$$\Psi_{vol}(J) = \frac{\kappa}{2}(J-1)^2, \quad (9)$$

where  $\kappa$  is a bulk modulus determined experimentally. This function is often used by most of FE codes.

Ogden proposed a volumetric response function in terms of the volume ratio  $J$  in the following form:

$$\begin{aligned} \Psi_{vol}(J) &= \kappa \mathcal{G}(J), \\ \mathcal{G}(J) &= \beta^{-2}(\beta \ln J + J^{-\beta} - 1), \\ \mathcal{G} &= \frac{1}{4}(J^2 - 1 - 2 \ln J) \text{ for } \beta = -2. \end{aligned} \quad (10)$$

#### The isotropic deviatoric part of strain energy function

Neo-Hookean, Mooney-Rivlin and Ogden models are commonly used :

$$\begin{aligned} \Psi_{iso} &= \frac{\mu}{2}(\bar{I}_1 - 3), \\ \Psi_{iso} &= c_{10}(\bar{I}_1 - 3) + c_{01}(\bar{I}_2 - 3), \\ \Psi_{iso} &= \Psi(\bar{\lambda}_1, \bar{\lambda}_2, \bar{\lambda}_3) = \sum_{a=1}^N \frac{\mu_a}{\alpha_a} (\bar{\lambda}_1^{\alpha_a} + \bar{\lambda}_2^{\alpha_a} + \bar{\lambda}_3^{\alpha_a} - 3). \end{aligned} \quad (11)$$

#### The anisotropic deviatoric part

We used the polynomial [3] and exponential functions of the anisotropic invariants  $\bar{I}_4, \bar{I}_5, \bar{I}_6, \bar{I}_7$  and  $\bar{I}_8$  :

$$\begin{aligned} \Psi_{ani} &= \sum_{i=2}^6 a_i (\bar{I}_4 - 1)^{2i} + \sum_{j=2}^6 b_j (\bar{I}_5 - 1)^{2j} + \sum_{k=2}^6 c_k (\bar{I}_6 - 1)^{2k} \\ &\quad + \sum_{l=2}^6 d_l (\bar{I}_7 - 1)^{2l} + \sum_{m=2}^6 e_m (\bar{I}_8 - \zeta)^{2m}, \end{aligned} \quad (12)$$

where  $a_i, b_j, c_k, d_l$  and  $e_m$  are material constants, and  $\zeta = (\mathbf{a}_0 \cdot \mathbf{b}_0)^2$ .

$$\Psi_{ani} = \frac{k_1}{2k_2} \left\{ \exp \left[ k_2 (\bar{I}_4 - 1)^2 \right] - 1 \right\} + \frac{k_1}{2k_2} \left\{ \exp \left[ k_2 (\bar{I}_6 - 1)^2 \right] - 1 \right\}, \quad (13)$$

where  $k_1 > 0$  is a stress-like material parameter and  $k_2 > 0$  is a dimensionless parameter.

## 4 Material model implementation into Comsol Multiphysics

The constitutive equations of material models were derived in Symbolic Toolbox of Matlab then inserted into Global Expressions and Subdomain Settings - Equation System tables. In Subdomain Settings we have redefined the free energy function (Fig.1)

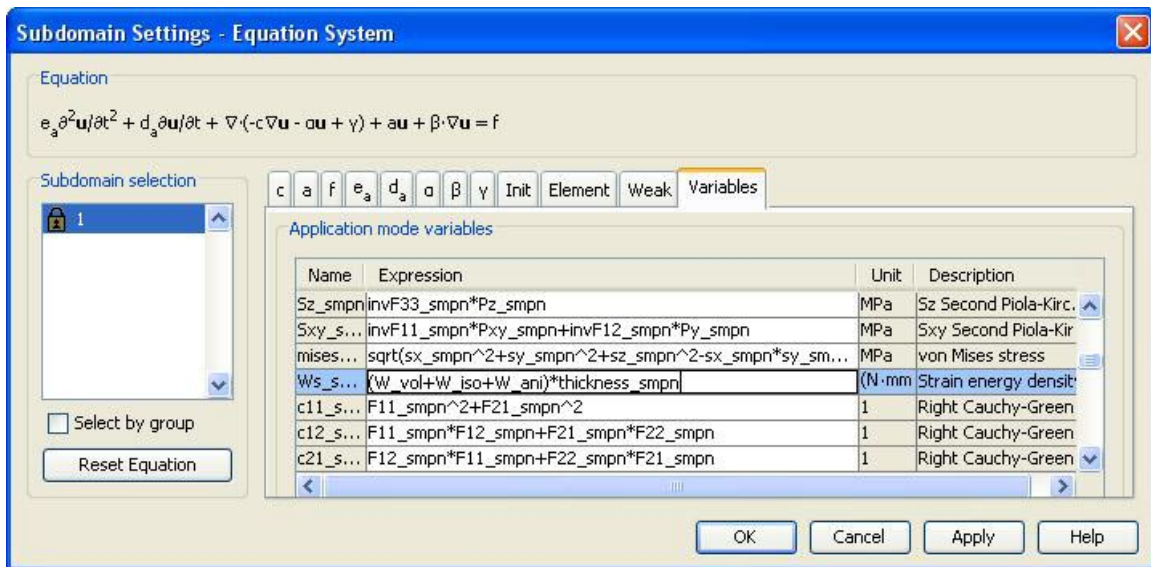


**Figure 1.** New free energy function

In Global Expressions table we defined the anisotropic strain energy function and all constitutive equations of material as well as the expressions for the calculation of principal stretches for Ogden's model (Fig.2). The detailed description of this part can be found in attached Comsol Report of our calculations.

## 5 Applications and examples

We verified our model by calculus of deformation and stress in a rectangular fiber-reinforced composite block in plane strain state with a centric circular hole. We combined different configurations of the reinforcement fibers and different constitutive material models.

The dimensions of the block are 20×20 mm and the radius of the hole  $r = 5$  mm. The block was loaded in tension by the displacement  $u_x$  at the right boundary (the  $y$  displacement here was  $u_y = 0$ ). The opposite left edge was fixed and the remaining boundaries were free.

We built the geometry and applied appropriately boundary conditions, we chosen automatic mesh method with maximum element size 0.7 mm (Fig.3).

Name	Expression	Unit	Description
I1	$C_{11}+C_{22}+C_{33}$	1	Invariants of...
I2	$0.5*(I_1^2-C_{11}^2-2*C_{12}^2-2*C_{13}^2-C_{22}^2-2*C_{23}^2-C_3...$	1	
I3	$J^2$	1	
II1	$I_1*I_3^{(-1/3)}$	1	Modified inva...
II2	$I_2*I_3^{(-2/3)}$	1	
II4	$A_1*(C_{11}*A_1+C_{12}*A_2+C_{13}*A_3)+A_2*(C_{21}*A_1+C_{22}*...$	1	
II6	$B_1*(C_{11}*B_1+C_{12}*B_2+C_{13}*B_3)+B_2*(C_{21}*B_1+C_{22}*B...$	1	
Lamd...	$1/2*C_{11}+1/2*C_{22}+1/2*(C_{11}^2-2*C_{11}*C_{22}+C_{22}^2+4*C...$	1	
Lamd...	$1/2*C_{11}+1/2*C_{22}-1/2*(C_{11}^2-2*C_{11}*C_{22}+C_{22}^2+4*C1...$	1	
Lamd...	$C_{33}$	1	
lamda1	$LamdaC_1^{0.5}$	1	
lamda2	$LamdaC_2^{0.5}$	1	
lamda3	$LamdaC_3^{0.5}$	1	
lamda_1	$J^{(-1/3)}*lamda1$	1	
lamda_2	$J^{(-1/3)}*lamda2$	1	
lamda_3	$J^{(-1/3)}*lamda3$	1	
W_vol	$K_b/4*(J^2-1-2*log(J))$	1	Volumetric st...
W_iso	$muy_1/a_1*(lamda_1^{a_1}+lamda_2^{a_1}+lamda_3^{a_1-3})+muy...$	1	Isochoric str...
W_ani	$k_1/(2*k_2)*(exp(k_2*(II_4-1)^2)-1)+k_1/(2*k_2)*(exp(k_2*(II_6-1...$	1	Anisotropic s...

Figure 2. Constitutive equations of the material model

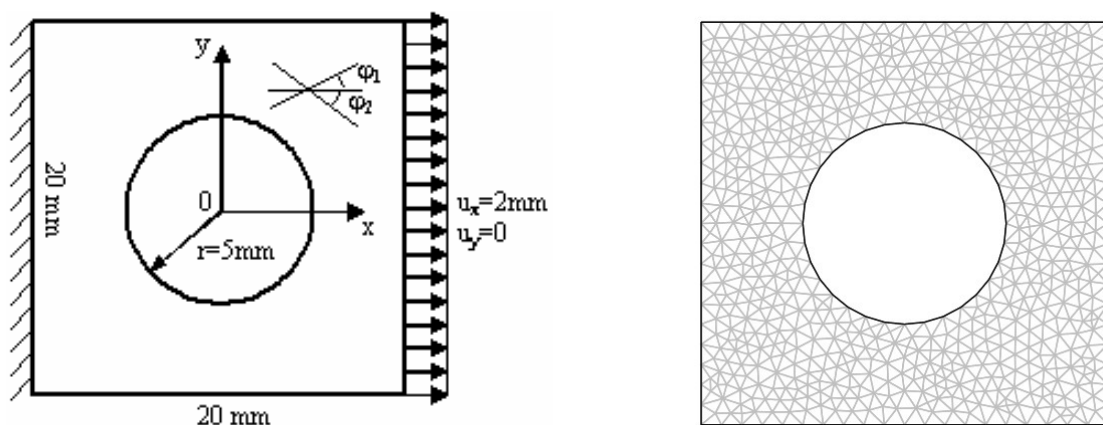


Figure 3. Geometry, mesh and boundary conditions

## One family of fiber

The free energy function used in this calculus was the combination of the simple volumetric function (9), the Mooney-Rivlin function (11<sub>2</sub>) and the polynomial anisotropic function (12) with only one term depending on the invariant  $\bar{I}_4$ . The directions of the fibers with respect to the loading axis were  $\varphi_1 = 0^\circ, 15^\circ, 30^\circ, 45^\circ$  and  $60^\circ$ .

The stress for the fiber direction  $\varphi=15^\circ$  is at Fig. 4 and the dependency of the maximum stress on the fiber angle is obvious from Fig.5. The direction of fibers affects strongly the distribution and magnitude of the stress.

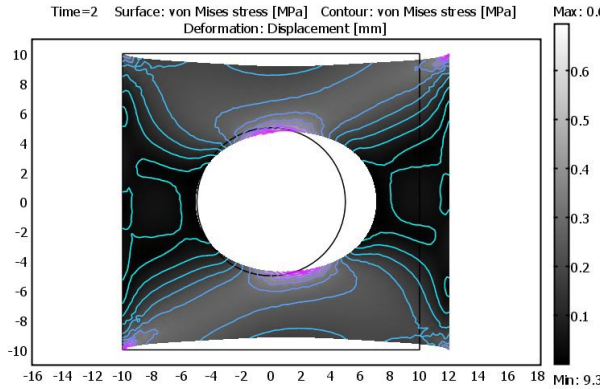


Figure 4. Deformation and stress for  $\varphi=15^\circ$

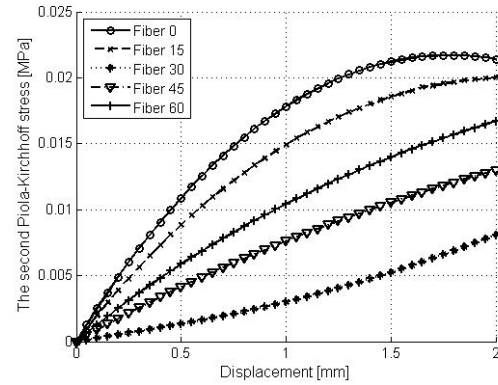


Figure 5. Stress dependent on fiber direction

## Two perpendicular families of fibers

In this case the two families of fibers are perpendicular mutually and contain different angles with the loading direction. The volumetric and isotropic parts of strain energy function were chosen the same as in previous case. The polynomial anisotropic function (12) depends here on the two invariants  $\bar{I}_4$  and  $\bar{I}_6$ . The directions of the fibers were  $\varphi_1 = 0^\circ, 15^\circ, 30^\circ$  and  $45^\circ$ .

It is obvious from the results at Fig. 6 and 7 that the distribution and the magnitude of the stress depend largely on the fibers direction. The ability of the plate to undergo loading is higher than for the plate with one family of fiber. If the fibers are arranged symmetrically with respect to the axis of loading the structure is very supple.

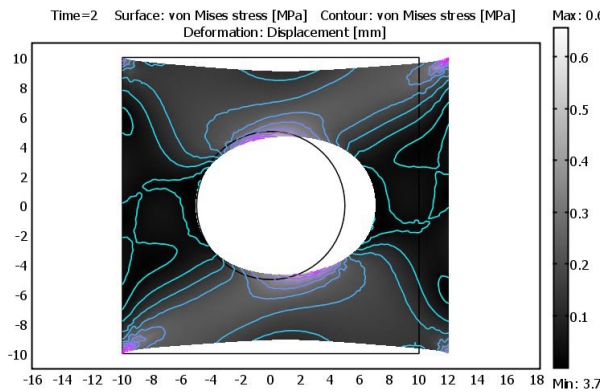


Figure 6. Deformation and stress for  $\varphi=30^\circ$

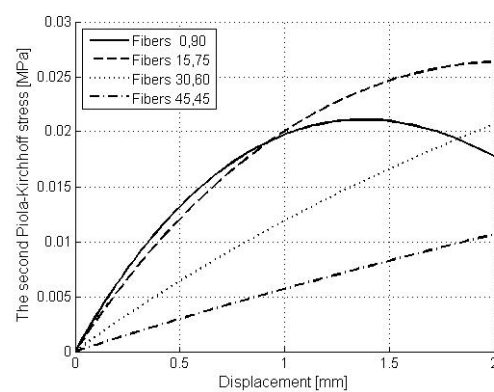


Figure 7. Stress dependent on fiber direction

## Two families of fibers arranged symmetrically with respect to the axis of loading

We used the same material model and material constants as for the two families of perpendicular fibers. In this case we can calculate only a quarter of the model and apply symmetric boundary conditions. The directions of the fibers were  $\varphi_1=\varphi_2=15^\circ, 30^\circ, 45^\circ$  and  $60^\circ$ . The results are at Fig. 8 and 9.

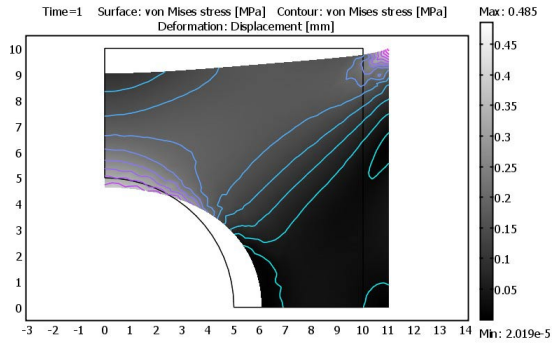


Figure 8. Deformation and stress for  $\varphi=45^\circ$

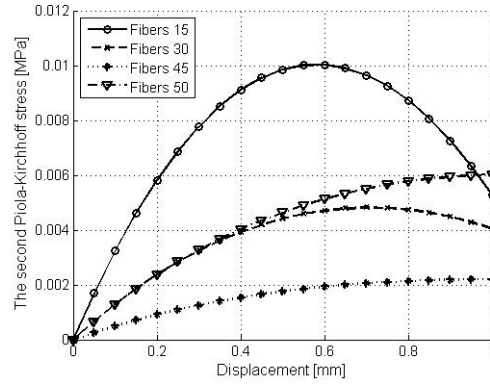


Figure 9. Stress dependent on fiber direction

## Comparison of different material models

In previous examples we used the volumetric function (9) Mooney-Rivlin model (11<sub>2</sub>) for the isotropic part and the polynomial model (12) for the anisotropic part of the free energy function. Now we compare different combinations of volumetric, isotropic and anisotropic parts.

### One family of fiber with the direction $\varphi = 30^\circ$

The volumetric function and the anisotropic function are given by (9) and (12) respectively and the isotropic parts are in sequence Neo-Hookean, Mooney-Rivlin and Ogden models (11). The results are at the Fig. 10.

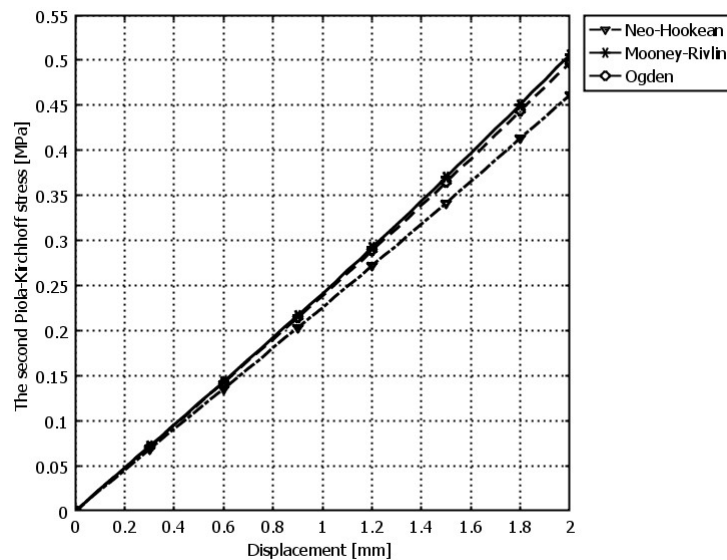


Figure 10. Stress and displacement with Neo-Hookean, Mooney-Rivlin and Ogden models

## Two families of fibers with the directions $\varphi_1 = \varphi_2 = 45^\circ$

We chose the following combinations with  $\Psi_{ISO}$  as Ogden model (11<sub>3</sub>)

- Model 1:  $\Psi_{VOL}$  given by eq. (9),  $\Psi_{ANI}$  polynomial expression (12)
- Model 2:  $\Psi_{VOL}$  given by eq. (10<sub>3</sub>),  $\Psi_{ANI}$  polynomial expression (12)
- Model 3:  $\Psi_{VOL}$  given by eq. (9),  $\Psi_{ANI}$  exponential expression (13)
- Model 4:  $\Psi_{VOL}$  given by eq. (10<sub>3</sub>),  $\Psi_{ANI}$  exponential expression (13)

The comparison of results is at Fig. 11. It can be seen that there is not the substantial difference between particular models.

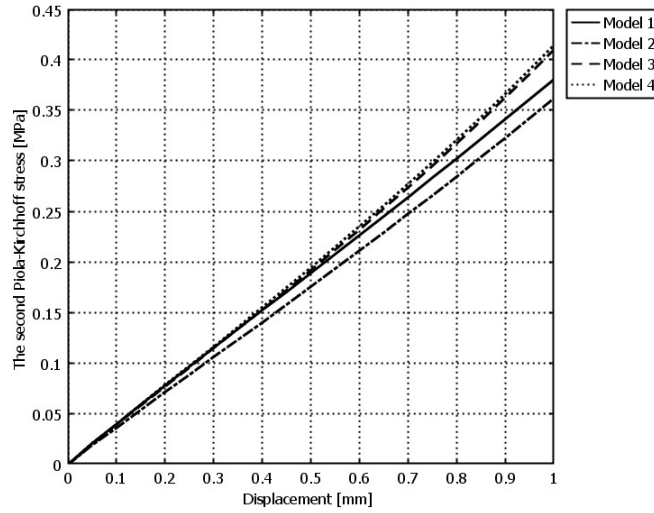


Figure 11. Stress and displacement with different models

## 6 Conclusion

The new material model of the anisotropic composite material in finite strain and the Ogden model of hyperelastic material in 2-D were implemented into Comsol Multiphysics. Some simple examples were subsequently presented, namely the extension of a composite block with a central hole. The material of the block was modeled using anisotropic hyperelastic constitutive equations. The effect of different configurations of the reinforcing fibers is demonstrated. The alternation of the fiber parameters resulted in a variety of stress distribution in the composite block. The influence of different models for the volumetric, isotropic and anisotropic parts of the Helmholtz free energy function was also examined and displayed. The results are in qualitative agreement with experimental observations.

### *Acknowledgement:*

This work was supported by the subvention from Ministry of Education of the Czech Republic under Contract Code MSM 4674788501



## References

- [1] Holzapfel, G.A. *Nonlinear Solid Mechanics. A Continuum Approach for Engineering*, John Wiley & Son, Chichester, 2000.
- [2] Holzapfel, G.A, Gasser, T.C. *A viscoelastic model for fiber-reinforced composites at finite strains: Continuum basis, computational aspects and applications*. *Computer Methods in Applied Mechanics and Engineering*, Vol. 190, 4379-4430, 2001.
- [3] Tran Huu Nam, *Mechanical properties of the composite material with elastomeric matrix reinforced by textile cords*, Ph.D Thesis, Technical University of Liberec, 2004.